

# Dynamic block displacement prediction – validation of DDA using analytical solutions and shaking table experiments

M. Tsesarsky & Y. H. Hatzor

*Department of Geological and Environmental Sciences, Ben Gurion University of the Negev, Beer – Sheva, 84105, Israel*

N. Sitar

*Department of Civil Engineering, University of California, Berkeley, CA94720, USA*

**ABSTRACT:** The accuracy and validity of Discontinuous Deformation Analysis (DDA) is tested using analytical solutions and shaking table experiments. The displacement history of a single block on an inclined plane subjected to a sinusoidal loading function, with input frequencies ranging from 2.66 Hz to 8.6 Hz, is studied. DDA predicts accurately the measured displacements and its evolution with time. Sensitivity analyses of the numeric control parameters show: 1) Artificial numeric damping is required if better accuracy is sought. For the case of a single block on an incline a reduction of the dynamic control parameter by 2% is recommended; 2) Accurate DDA solution is attained for high penalty (numeric spring stiffness) values, provided that the chosen time step is small enough to assure diagonal dominance of the global stiffness matrix; 3) For a given time step size a sensitivity analysis of the numeric spring stiffness should be performed to detect ill conditioning or loss of diagonal dominance.

## 1 INTRODUCTION

Discontinuous Deformation Analysis (DDA) (Shi, 1988; 1993) is a numeric model for analyzing statics and dynamics of discontinuous block systems. Successful application of the DDA method to various engineering problems requires rigorous validation. The accuracy of DDA has been tested by many researchers. Yeung (1991) and MacLaughlin (1997) tested the accuracy of DDA for applications ranging from tunneling to slope stability, using problems for which analytical or semi-analytical solutions exist. Doolin and Sitar (2001) explored the kinematics of a block on an incline for sliding distances of up to 250 meters. Hatzor and Feintuch (2001) validated DDA using direct dynamic input. Analytical integration of sinusoidal functions of increasing complexity was compared to displacements prescribed by DDA for a single block on an incline subjected to the same acceleration functions as integrated analytically.

The necessity for DDA validation using analytical solutions is evident if the method is to be adopted by the engineering profession. However, analytical solutions are only valid for the inherent underlying simplifying assumptions. This limitation can be overcome by comparison between DDA prediction and experimental results of carefully planned physical models. Up to date, such attempts have been limited, or practically non-existent for the dynamic problem.

O'sullivan and Bray (2001) simulated the behavior of hexagonally packed glass rods subjected to biaxial compression, showing the advantages of DDA in the study of soil dynamics. McBride and Scheele (2001) validated DDA using a multi-block array on an incline subjected to gravitational loading, and a bearing capacity model.

Validation of DDA using analytical solutions (Yeung, 1991; MacLaughlin, 1997; Doolin and Sitar, 2001; Hatzor and Feintuch, 2001) showed that DDA accurately predicts single block displacements, up to tens of meters. However, validation using physical models proves less successful. In particular, it is found that kinetic damping is required for reliable prediction of displacement (McBride and Scheele, 2001).

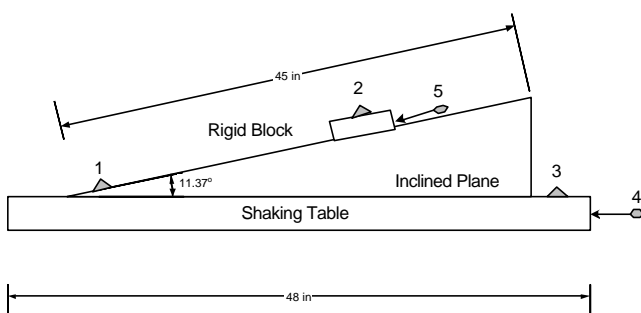
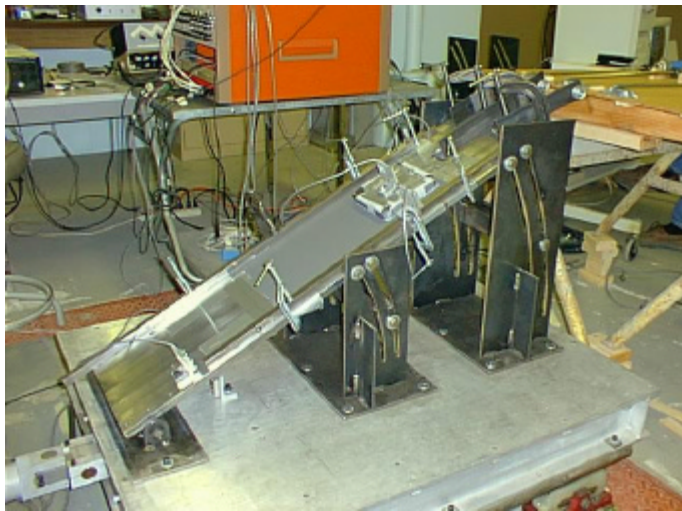
In this paper we study the displacement history of a single block on an incline subjected to dynamic loading. The following issues are addressed:

1. Comparison between DDA solution and results of a physical model.
2. Sensitivity analyses of the numeric control parameters: numeric spring stiffness ( $g0$ ), time step size ( $g1$ ), assumed maximum displacement ratio ( $g2$ ), and the dynamic control parameter ( $k01$ ).
3. The nature and evolution of the computational error.

## 2 EXPERIMENTAL SETTINGS

The physical modeling used in this research was performed by Wartman (1999) at the Earthquake Simulation Laboratory of the University of California at Berkley. The tests were performed on a large hydraulic driven shaking table, producing accurate, well controlled, and repeatable motions to frequencies up to 14 Hz. The table was driven by a 222.4 kN (50 kip) force, 15.24 cm (6 in.) hydraulic actuator range manufactured by MTS. The system was closed loop servo controlled. A Hewlett Packard 33120A arbitrary function generator produced the table command signal.

The physical modeling used in this research was performed by Wartman (1999) at the Earthquake Simulation Laboratory of the University of California at Berkley. The tests were performed on a large hydraulic driven shaking table, producing accurate, well controlled, and repeatable motions to frequencies up to 14 Hz. The table was driven by a 222.4 kN (50 kip) force, 15.24 cm (6 in.) hydraulic actuator range manufactured by MTS. The system was closed loop servo controlled. A Hewlett Packard 33120A arbitrary function generator produced the table command signal.



No.	Instrument	Direction of Measurement
1	accelerometer	parallel to plane
2	accelerometer	parallel to plane
3	accelerometer	horizontal
4	displacement transducer	horizontal
5	displacement transducer	parallel to plane

Figure 1. a) General view of the inclined plane and the sliding block (top); b) Sliding block experimental setup and instrumentation location (bottom). Source: Wartman (1999).

An inclined steel plane was fitted to the shaking table. The plane inclination was set to  $11.37^\circ$  during the rigid block tests. The steel rigid block was 2.54 cm (1 in.) thick, with area of  $25.8 \text{ cm}^2$  (4 in.<sup>2</sup>), and weight of 1.6 kg (3.5 lbs). Linear accelerometers were fitted on top of the sliding block and the inclined plane. Displacement transducers measured the relative displacement of the sliding block, and of the shaking table (Fig. 1)

Geotextile and geomembrane were fitted to the face of the sliding block and the inclined plane respectively. The static friction angle ( $f$ ) of the interface was determined using tilt tests and a value of  $f = 12.7^\circ \pm 0.7^\circ$  was reported. Kim et al., (1999) found that the geotextile – geomembrane interface friction exhibited pronounced strain rate effects, and reported an increase by 20% over a log-cycle of strain rate. Wartman (1999) showed that the friction angle of the interface was controlled by two factors: 1) amount of displacement; and 2) sliding velocity. For the range of velocities and displacements attained at the shaking table experiments the back-calculated friction angle was in the range of  $\phi = 14^\circ - 19^\circ$  (Fig. 2).

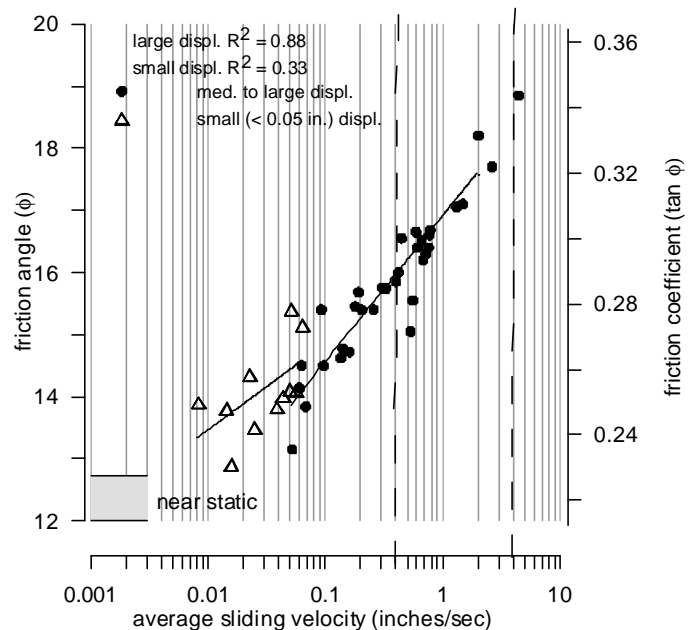


Figure 2. Back analyzed friction angles as a function of average sliding velocity for the rigid block tests, from Wartman (1999).

At its present stage of development DDA accepts a constant value of friction angle. Therefore a representative value of friction angle ( $\phi_{av}$ ) should be chosen for the validation study. The value of  $f_{av}$  was determined as follows. First, the measured displacement of the block was differentiated with respect to time and hence the velocity record was attained. Next, the velocity content was computed. Taking as an example, the 2.66 Hz input motion frequency test showed that the velocity upper bound value was below 10 cm/sec (4 in/sec), refer to Figure 3a. This value was attained only for

short periods of time during the test. The velocity content chart shows that 70% of the velocities fall under the value of 2.54 cm/sec (1 in/sec), refer to Figure 3b. Taking the value of 2.54 cm/sec as the upper bound velocity, the corresponding friction angle is  $f_{av} < 17^\circ$ , while  $f_{av} = 16^\circ$  is the most likely value.

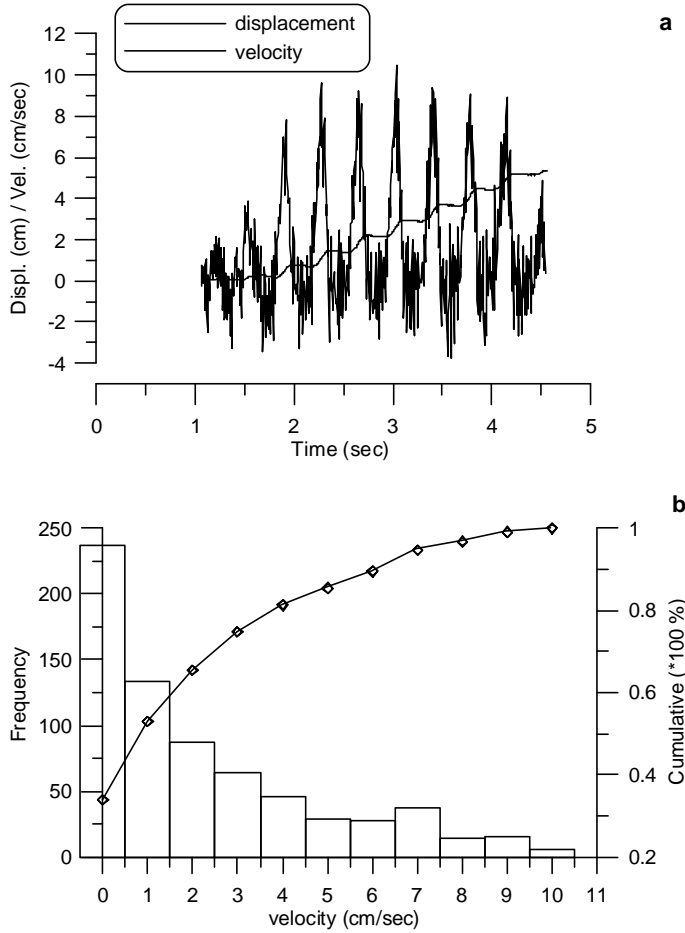


Figure 3. a) Displacement derived velocity, 2.66 Hz frequency sinusoidal input test; b) Velocity content of the 2.66 Hz frequency sinusoidal input test.

In this study sinusoidal input motion tests were used for validation. A Typical sinusoidal input motion is shown in Figure 4. The motion was ramped up linearly for 1.5 seconds to insure shaking table stability, followed by full amplitude for duration of 2 seconds, and finally ramped down for 1.5 seconds. Eight different tests were used for validation (Tab. 1).

Table 1. Input motion summary:  $\omega$  is the input motion frequency,  $d_T$  is the shaking table displacement,  $d_B$  is relative block displacement, and  $a_h$  is maximum horizontal table acceleration.

Test	$\omega$ Hz	$d_T$ cm	$d_B$ cm	$a_h$ g
1	2.66	0.889	5.367	0.28
2	4	0.559	6.604	0.25
3	5.33	0.305	3.341	0.19
4	6	0.254	3.647	0.19
5	6.67	0.254	3.410	0.22
6	7.3	0.228	3.353	0.22
7	8	0.228	3.937	0.23
8	8.66	0.019	2.882	0.21

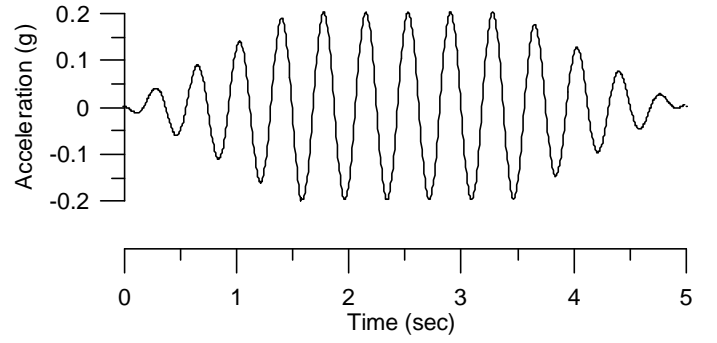


Figure 4. Shaking table typical sinusoidal input motion, 2.66 Hz frequency (Test 1 at Table 1)

### 3 DDA FUNDAMENTALS AND NUMERICAL SETTINGS

#### 3.1 DDA formulation

DDA models a discontinuous material as a system of individually deformable blocks that move independently without interpenetration. In the DDA method the formulation of the blocks is very similar to the definition of a finite element mesh. A finite element type of problem is solved in which all elements are physically isolated blocks bounded by pre-existing discontinuities. The blocks used in DDA can assume any given geometry, as oppose to the predetermined topologies of the FEM elements.

DDA first order displacement approximation assumes that each block is a constant strain/stress element. The displacements ( $u, v$ ) at any point ( $x, y$ ) in a block  $i$ , can be related in two dimensions to six displacement variables

$$[D_i] = (u_0 \quad v_0 \quad r_0 \quad e_x \quad e_y \quad \gamma_{xy})^T \quad (1)$$

where ( $u_0, v_0$ ) is the rigid body translations of a specific point ( $x_0, y_0$ ) within a block, ( $r_0$ ) is the rotation angle of the block with a rotation center at ( $x_0, y_0$ ), and  $e_x, e_y$  and  $\gamma_{xy}$  are the normal and shear strains of the block. For a two-dimensional formulation of DDA, the center of rotation ( $x_0, y_0$ ) coincides with block centroid ( $x_c, y_c$ ). Shi (1988) showed that the complete first order approximation of block displacement takes the following form

$$\begin{pmatrix} u \\ v \end{pmatrix} = [T_i][D_i] \quad (2)$$

$$= \begin{bmatrix} 1 & 0 & -(y-y_0) & (x-x_0) & 0 & (y-y_0)/2 \\ 0 & 1 & (x-x_0) & 0 & (y-y_0) & (x-x_0)/2 \end{bmatrix} [D_i]$$

This equation enables the calculation of displacements at any point ( $x, y$ ) of the block when the displacements are given at the center of rotation and when the strains are known.

In DDA individual blocks form a system of blocks through contacts among blocks and displacement constrains on a single block. For a block system de-

defined by  $n$  blocks the simultaneous equilibrium equations are

$$\begin{pmatrix} K_{11} & K_{12} & K_{13} & \Lambda & K_{1n} \\ K_{21} & K_{22} & K_{23} & \Lambda & K_{2n} \\ K_{31} & K_{32} & K_{33} & \Lambda & K_{3n} \\ M & M & M & O & M \\ K_{n1} & K_{n2} & K_{n3} & \Lambda & K_{nn} \end{pmatrix} \begin{Bmatrix} D_1 \\ D_2 \\ D_3 \\ M \\ D_n \end{Bmatrix} = \begin{Bmatrix} F_1 \\ F_2 \\ F_3 \\ M \\ F_n \end{Bmatrix} \quad (3)$$

where  $K_{ij}$  are  $6 \times 6$  sub-matrices defined by the interactions of blocks  $i$  and  $j$ ,  $D_i$  is a  $6 \times 1$  displacement variables sub-matrix, and  $F_i$  is a  $6 \times 1$  loading sub-matrix. In total the number of displacement unknowns is the sum of the degrees of freedom of all the blocks. The diagonal sub-matrices  $K_{ij}$  represent the sum of contributing sub-matrices for the  $i$ -th block, namely block inertia and elastic strain energy. The off diagonal sub-matrices  $K_{ij}$  ( $i \neq j$ ) represent the sum of contributing sub-matrices of contacts between blocks  $i$  and  $j$  and other inter-element actions like bolting.

The simultaneous equations are derived by minimizing the total potential energy  $\Pi$  of the block system. The  $i$ -th row of (3) consists of six linear equations

$$\frac{\partial \Pi}{\partial d_{ri}} = 0, r = 1, 2, 3, 4, 5, 6 \quad (4)$$

where  $d_{ri}$  are the deformation variables of block  $i$ . Full detail of stiffness matrix and load vector assembly is found in Shi (1993).

The solution to the system of equations (3) is constrained by inequalities associated with block kinematics, no penetration and no tension condition between blocks. The kinematic constraints on the system are imposed using the penalty method. Contact detection is performed in order to determine possible contacts between blocks. Numerical penalties analogous to stiff springs are applied at the contacts to prevent penetration. Tension or penetration at the contacts results in expansion or contraction of the ‘‘springs’’, which adds energy to the block system. Thus the minimum energy solution is one with no tension or penetration. When the system converges to an equilibrium state the energy of the contact forces is balanced by the penetration energy, resulting in inevitable very small penetrations. The energy of the penetrations is used to calculate the contact forces, which are in turn used to calculate the frictional forces along the interfaces between blocks. Shear displacement along the interfaces is modeled using Coulomb - Mohr failure criterion. Fixed boundary conditions are enforced in a manner consistent with the penalty method formulation. Stiff springs are applied at fixed points. Displacement of the fixed points adds considerable energy to the block system. Thus, a minimum energy solution sat-

isfies the no displacement condition of the fixed points.

The solution of the system of equations is iterative. First, the solution is checked to see how well the constraints are satisfied. If tension or penetration is found along contacts the constraints are adjusted by selecting new position for the contact springs and a modified versions of  $[K]$  and  $\{F\}$  are formed for which a new solution is attained. The process is repeated until each of the contacts converges to a constant state. The positions of the blocks are then updated according to the prescribed displacement variables. The large displacements and deformations are the accumulation of small displacements and deformations at each time step.

DDA time integration scheme adopts the Newmark (1959) approach, which for a single degree of freedom can be written in the following manner:

$$\begin{aligned} u_{i+1} &= u_i + \Delta t \dot{u}_i + \left(\frac{1}{2} - \mathbf{b}\right) \Delta t^2 \ddot{u}_i + \mathbf{b} \Delta t^2 \ddot{u}_{i+1} \\ \dot{u}_{i+1} &= \dot{u}_i + (1 - \mathbf{g}) \Delta t \ddot{u}_i + \mathbf{g} \Delta t \ddot{u}_{i+1} \end{aligned} \quad (5)$$

where  $\ddot{u}$ ,  $\dot{u}$ , and  $u$  are acceleration, velocity, and displacement respectively,  $\Delta t$  is the time step,  $\mathbf{b}$  and  $\mathbf{g}$  are the collocation parameters defining the variation of acceleration over the time step. Unconditional stability of the scheme is assured for  $2\mathbf{b} \geq \mathbf{g} \geq 0.5$ . DDA integration scheme uses  $\mathbf{b} = 0.5$  and  $\mathbf{g} = 1$ , thus setting the acceleration at the end of the time step to be constant over the time step. This approach is implicit and unconditionally stable.

### 3.2 Numerical implementation of DDA

Computer implementation of DDA allows control over the analysis procedure through a set of user specified control parameters. The control parameters are:

1. Dynamic control parameter ( $k0I$ ) – defines the type of the analysis required, from static to fully dynamic. For static analysis the velocity of each block is set to zero at the beginning of each time step,  $k0I = 0$ . In the case of the dynamic analysis the velocity of each block at the end of a time step is fully transferred to the next time step,  $k0I = 1$ . Different values from 0 to 1 correspond to different degrees of damping or energy dissipation.
2. Penalty value ( $g0$ ) – is the stiffness of the contact springs used to enforce contact constraints between blocks.
3. Upper limit of time step size ( $gI$ ) – the maximum time interval that can

be used in a time step, should be chosen so that the assumption of infinitesimal displacement within the time step is satisfied.

4. Assumed maximum displacement ratio ( $g_2$ ) – the calculated maximum displacement within a time step is limited to an assumed maximum displacement in order to ensure infinitesimal displacements within a time step. The assumed maximum displacement is defined as  $g_2 \cdot (h/2)$ , where  $h$  is the length of the analysis domain in the y-direction.  $g_2$  is also used to detect possible contacts between blocks.

In this study the recently developed C/PC version of DDA (Shi, 1999) is used. In this version, dynamic acceleration can be input directly, and updated at every time step. A necessary condition for direct input of dynamic acceleration is that the numerical computation has no artificial damping because artificial damping may lead to energy losses. In DDA the solution of the equilibrium equations is performed without damping.

## 4 RESULTS OF VALIDATION STUDY

### 4.1 DDA calculation vs. Analytical Model

A Fourier series composed of sine components represents the simplest form of harmonic oscillations, in general notation:

$$a(t) = \sum_{i=1}^n a_i \sin(\mathbf{w}_i t) \quad (6)$$

where  $a_i$  and  $\mathbf{w}_i$  are the amplitude (acceleration in this case) and frequency respectively.

The displacement of a mass subjected to dynamic loading is attained by double integration of the acceleration record (Eq. 6) from  $\mathbf{q}$  to  $t$ :

$$d(t) = \sum_{i=1}^n \frac{a_i}{\mathbf{w}_i^2} [-\sin \mathbf{w}_i t + \sin \mathbf{w}_i \mathbf{q} + \mathbf{w}_i (t - \mathbf{q}) \cos \mathbf{w}_i \mathbf{q}] \quad (7)$$

where  $\mathbf{q}$  is the time at which yield acceleration  $a_y$  is attained. Goodman and Seed (1965) showed that for frictional sliding of a single block on a cohesionless plane the down slope horizontal yield acceleration is  $a_y = \tan(\mathbf{f} - \mathbf{a})g$ , where  $\mathbf{f}$  is the friction angle and  $\mathbf{a}$  is the plane inclination.

Hatzor and Feintuch (2001) showed that for an acceleration function consisting of sum of three sines DDA prediction are accurate within 15% of the analytic solution, provided the numeric control parameters  $g_1$ ,  $g_2$  are carefully optimized, and without application of damping. Moreover, they argued that the influence of higher order terms in a series of sine function is negligible. Hatzor and Feintuch demon-

strated their validation for  $a_1 = \mathbf{w}_1 = 1$ ,  $a_2 = \mathbf{w}_2 = 2$ ,  $a_3 = \mathbf{w}_3 = 3$ . The prescribed values produce a low frequency dynamic input assuring nearly constant block velocity, which was attained at the beginning of the analysis (*ca.* 20% of elapsed time).

In order to attain a better understanding of the frequency effect upon the numerical solution we have extended the analysis to higher frequencies, constraining the peak horizontal acceleration to  $0.15g$ . A typical input motion of sum of three sines is presented in Figure 5a. The analysis was performed for a single block resting on a plane inclined  $\mathbf{a} = 15^\circ$  to the horizontal. The block material properties were: density = 2700 kg/m<sup>3</sup>, E = 5000 MPa, and  $\nu = 0.25$ . The friction angle of the sliding plane was set to  $\mathbf{f} = 15^\circ$ , thus the yield acceleration ( $a_y = 0$ ) was attained immediately at the beginning of analysis ( $\mathbf{q} = 0$  sec). Three different sets of frequencies were modeled (Tab. 2). Constant values of numeric spring stiffness  $g_0 = 1000$  MN/m, assumed maximum displacement ratio  $g_2 = 0.0075$ , and dynamic control parameter  $k_01 = 1$  were used.

Table 2. Frequency sets for sum of three sines input function.

Set	$\omega_1$ ( $\pi$ ), $a_1$ (g)	$\omega_2$ ( $\pi$ ), $a_2$ (g)	$\omega_3$ ( $\pi$ ), $a_3$ (g)
1	8, 0.1	4, 0.05	2, 0.025
2	10, 0.1	5, 0.05	2.5, 0.025
3	15, 0.1	7.5, 0.05	3.75, 0.025

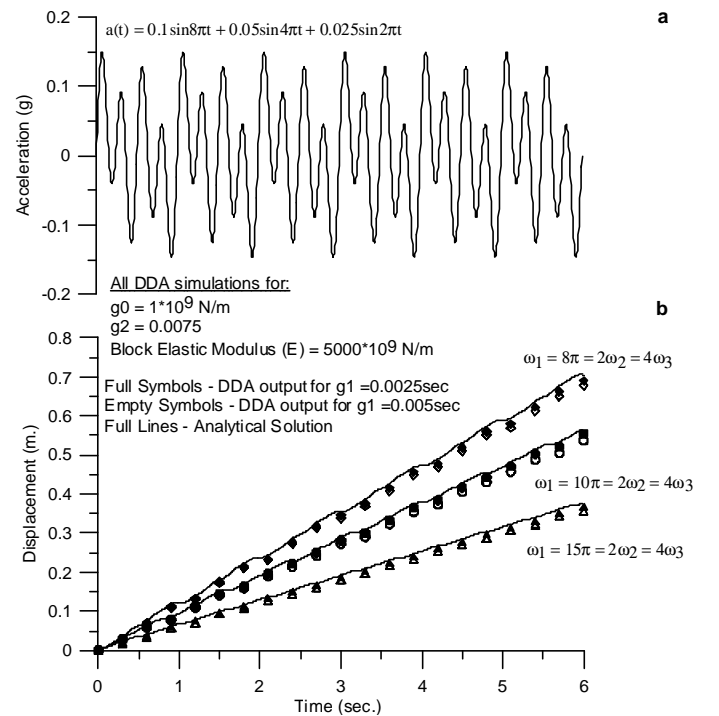


Figure 5. a) The loading function  $a(t) = a_1 \sin(\omega_1 t) + a_2 \sin(\omega_2 t) + a_3 \sin(\omega_3 t)$ ; b) Comparison between analytical and DDA solution for block displacement subjected to a sum of three sines loading function.

Each set was modeled twice, first the time step was set to  $g_1 = 0.005$  sec, then the time step was halved to  $g_1 = 0.0025$  sec. Comparison of analytical solution and numerical estimate of the total displacement are presented in Figure 5b, generally

showing excellent agreement between the analytical solution and the DDA solution, regardless of the frequency set chosen.

The absolute numeric error was defined in a conventional manner

$$E_N = \left| \frac{\|d\| - \|d_N\|}{\|d\|} \right| \quad (\%) \quad (8)$$

where  $d$  and  $d_N$  are the analytical and the numeric displacement vectors respectively.  $\|\cdot\|$  is the norm operator, which for a 2-D displacement vector is

$$\|d\| = \sqrt{u^2 + v^2}.$$

The numeric error for  $g1 = 0.005 \text{ sec}$  simulations is within 4.5% (Figure 5). Halving the time step reduces the numeric error to 1.5%.

We have further investigated the interrelationship of the numeric control parameters using the input function of set 2 (Table 2). Figure 6 shows the dependence of the numeric error on the choice of the numeric control parameters  $g1$ ,  $g2$  and the numeric spring stiffness  $g0$  (penalty value). It is found that for an optimized set of  $g1$  and  $g2$  ( $g1 = 0.0025 \text{ sec}$  and  $g2 = 0.0075$ ) the DDA solution is not sensitive to the penalty value, which can be changed over a range of two orders of magnitude. Within this range the numeric error never exceeds 10% and in most cases approaches the value of 1%. Naturally, stiffer contact springs reduce the magnitude of displacement until a certain minimum is reached. Further increase in the spring stiffness results in an introduction of a large numeric error into the DDA solution.

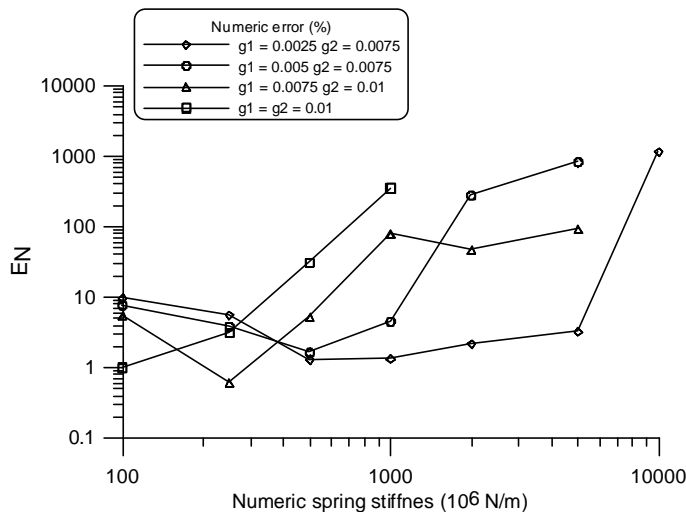


Figure 6. Absolute numeric error of DDA ultimate displacement prediction as a function of spring stiffness, for a sum of three sines loading function.

Departing from the optimal  $g1$ ,  $g2$  combination results in increased sensitivity of the DDA solution to the penalty value. The departure from the analytical solution occurs at lower penalty values with increasing time step size.

#### 4.2 DDA calculation vs. shaking table experiments

It has been showed that there is a very good agreement between the DDA and analytic solutions for the e block on an incline problem. However, the analytical solution is only an approximation of the physical problem with various simplifying assumptions including: perfectly rigid block, constant friction, and complete energy conservation. Comparison between DDA results and physical modeling can help us probe into the significance of these assumptions

The frictional properties of the geotextile – geomembrane interface are strain rate dependent as discussed above. Based on the criteria described earlier the upper bound for interface friction angle was  $f_{av} < 17^\circ$ , with the  $f_{av} = 16^\circ$  being the most likely value. Consequently, the DDA analyses were performed for friction angle values of  $f_{av} = 17^\circ$  and  $f_{av} = 16^\circ$ . The numeric control parameters for the two friction configurations were: penalty value  $g0 = 500 \cdot 10^6 \text{ N/m}$ , time step size  $g1 = 0.0025 \text{ sec}$ , assumed maximum displacement  $g2 = 0.005$ .

2.66 Hz input motion is discussed here in detail and the comparison results are shown in Figure 7.

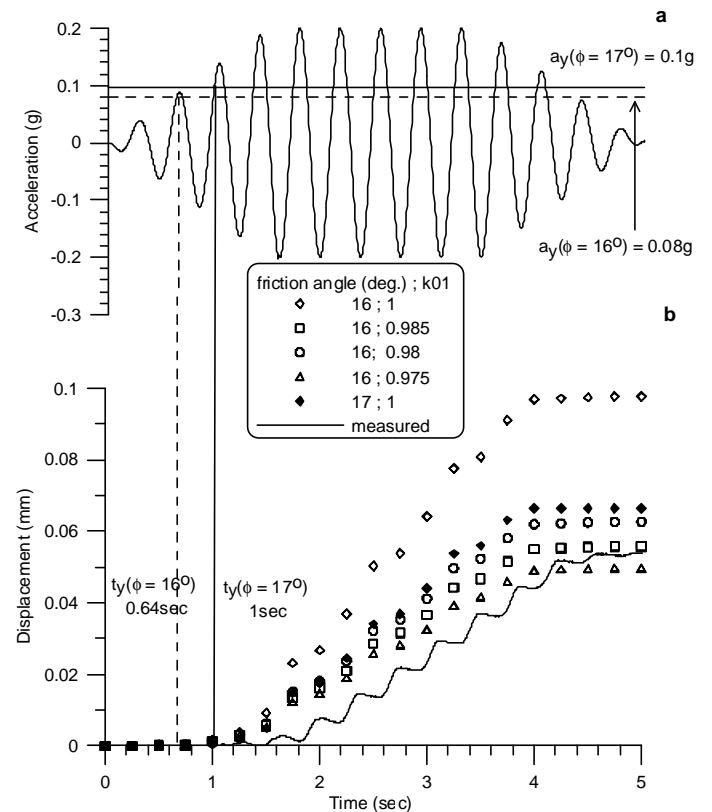


Figure 7. a) Physical model sinusoidal input function, 2.66 Hz frequency; b) Comparison of measured displacement and DDA solution.

With dynamic control parameter  $k01 = 1$  the DDA solution for  $f_{av} = 17^\circ$  falls within 20% of the measured displacement (Figure 8). Furthermore, the DDA solution captures the major features of the displacement history. The onset of displacement for  $f_{av} = 17^\circ$  is at  $a_y = 0.0985g$  according to the analytical solution of

Goodman and Seed (1965). This result is contemporary with both the DDA calculation and the measured record of displacement. When the acceleration falls below the yield value the block eventually stops. This behavior is captured by the DDA computation as well.

Setting  $f_{av} = 16^\circ$  reduces the accuracy of the DDA solution and the numeric error increases to approximately 80% (Fig. 8), but the ultimate displacement values are close, 0.055 m measured displacement compared to 0.093 m of calculated solution.

Introducing some kinetic damping by reducing  $k01$  below 1 improves the agreement between DDA and the physical test. Setting  $k01 = 0.985$ , corresponding to 1.5% velocity reduction, reduces the error to below 10%. Furthermore, reduction of  $k01$  improves the tracking of the displacement history by DDA.

Plotting the relative numeric error (a non absolute version of Eq. 4) against the input motion frequency (Fig. 9) shows that in general DDA accuracy increases with higher frequencies, with the exception at 6 Hz. For  $f_{av} = 16^\circ$  and  $k01 = 1$  the numeric error is always conservative, with the exception at 6 Hz. Reducing  $k01$  to 0.98 shows a similar effect for all frequencies, reducing the numeric error below 10%.

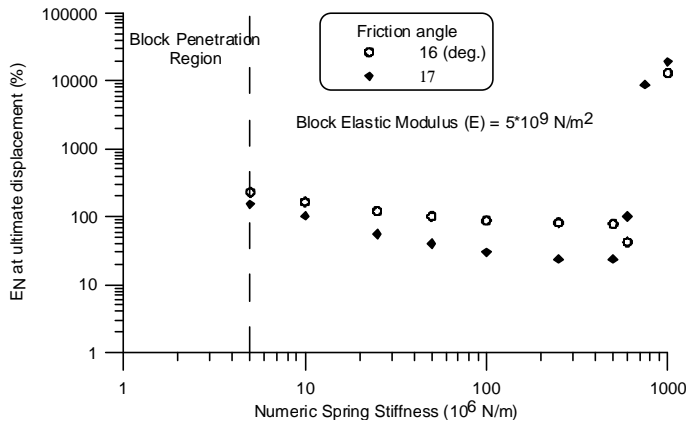


Figure 8. Absolute numeric error of DDA ultimate displacement prediction as a function of spring stiffness, for a sinusoidal input function. All DDA solutions for time step  $g1 = 0.0025 \text{ sec}$ , and assumed displacement ratio  $g2 = 0.005$ , dynamic control parameter  $k01 = 1$ .

## 5 DISCUSSION

The implicit formulation of DDA guarantees numerical stability regardless of time step size. However, it does not guaranty accuracy. Where the time step is too large or too small relative to the numeric spring stiffness, loss of diagonal dominance and/or ill conditioning error may result, interfering with convergence to an accurate solution. With the penalty method, employed to prevent block penetration or tension between blocks, the theoretical solution is approached only when the penalty value approaches infinity. Nevertheless, too large penalty values may result in errors due to lack of diagonal dominance and/or ill-conditioning.

The numeric implementation of DDA utilizes the SOR Gauss – Seidel equation solver. The convergence of the SOR equation solver is guaranteed for diagonally dominant matrices:

$$|K_{ii}| > \sum_{\substack{j=1 \\ j \neq i}}^n |K_{ij}| \quad (9)$$

Larger inertia terms on the diagonal of the global stiffness matrix increase the stability of the computation. A small time step size is needed to increase the inertia terms, which are inversely proportional to the square of time step. This effect can be seen in Figure 6. For small time steps (0.0025 sec) the numeric error does not exceed 10% for increasing penalty values up to  $5 \cdot 10^{10} \text{ N/m}$ , higher values introduce significant error as the off diagonal sub-matrices become larger, resulting in loss of diagonal dominance. Enlarging the time step results in reduction of the inertia term in the diagonal sub-matrices. Thus, for a given value of time step size the loss of diagonal dominance will occur at lower penalty values.

Figure 8 shows the accuracy of the DDA solution for different penalty values, for a given values of  $g1$  and  $g2$ . When the penalty is lower than  $5 \cdot 10^6 \text{ N/m}$  inter-block penetration occurs. For penalty values of  $5 \cdot 10^6 \text{ N/m}$  and up to  $600 \cdot 10^6 \text{ N/m}$  the accuracy of the solution is well confined between relatively narrow error margins. With  $f_{av} = 17^\circ$  the error is reduced from 110% to 20% over the studied range of penalties. Similarly, with  $\phi_{av} = 16^\circ$  the error is reduced from 120% to 80% over the same penalty range. When the penalty is exceedingly high an abrupt accumulation of error occurs due to loss of diagonal dominance of the global stiffness matrix or due to matrix ill conditioning.

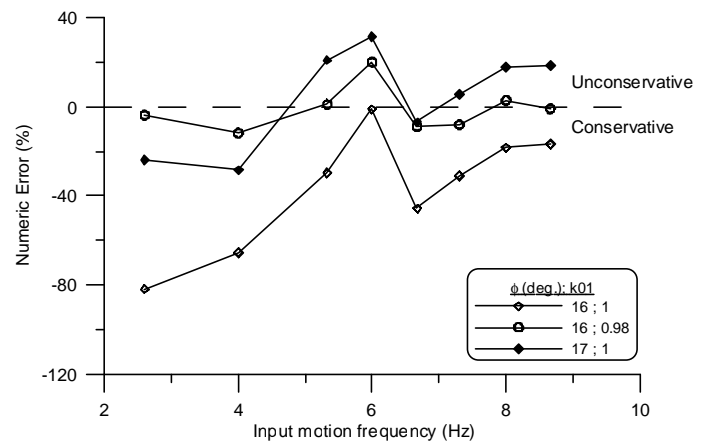


Figure 9. Numeric error of DDA ultimate displacement prediction as a function of input frequency, for a sinusoidal input function

Most of the error is accumulated at the beginning of the analysis and it declines with time, a phenomenon known as algorithmic damping (Figure 10). Similar observations were reported by Doolin and Sitar (2001) for the case of a gravity driven block. The



maximum error value is a test artifact associated with the transition from a ramped motion to a steady sine input motion in the shaking table experiment and can be ignored. This trend is maintained here for all values of  $kOI$  selected; greater accuracy is attained when  $kOI$  is optimized. Algorithmic damping is typical to implicit time integration schemes. In DDA, a Newmark type implicit, time integration scheme (collocation parameters are  $\mathbf{b} = \mathbf{0.5}$ ,  $\mathbf{d} = \mathbf{1}$ ) assures unconditional stability of integration and high algorithmic damping (Wang et al., 1996). Thus, damping is performed without the introduction of energy consuming devices. The amount of algorithmic damping depends on the time integration method, the time step size, and the natural period of the system.

In this study we have limited the duration of the analysis to 5 seconds, in conjunction with the physical model. It has been shown that algorithmic damping reduces the numeric error as calculation evolves. Doolin and Sitar (2001) showed that error reduction is evident for sliding distances of up to 250m over 16 sec. Thus, for larger time spans the error will decline with calculation progress to a certain minimum value, further improving solution accuracy.

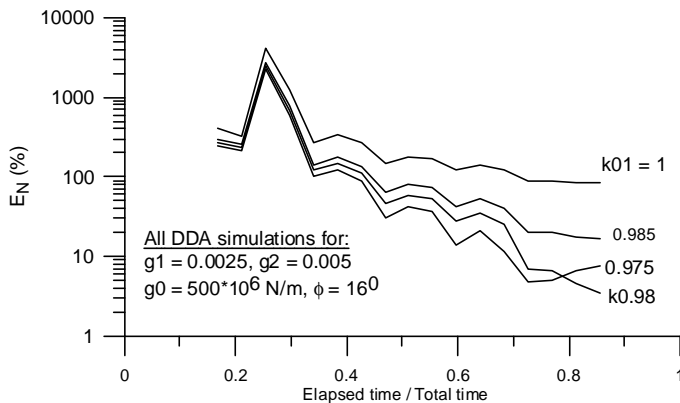


Figure 10. Numeric error evolution of DDA solution for sinusoidal input function at 2.66 Hz input frequency.

Dynamic formulation of DDA is essentially undamped, thus for evolving systems the only way to dissipate energy is by frictional resistance. The physical model is however more complicated, energy losses through structural vibrations, heat radiation, drag, and other physical mechanisms are present, and not accounted for by DDA. Reduction of the transferred velocity at each time step reduces the overall dynamic behavior of the discrete system without imposing ill-conditioning of the stiffness matrix (Wang et al., 1996). In a similar manner a quasi-static analysis is performed by setting  $kOI = 0$ . Thus we recommend that for full-scale simulations a certain amount of kinetic damping should be applied.

McBride and Scheele (2001) showed similar effect for a gravity driven multi-block structure,

showing that optimal results were achieved for  $kOI = 0.8$ . It is reasonable to assume that higher kinetic damping is required for multi-block structures, to account for a large number of contacts and block interactions. However, this estimate should be examined in conjunction with the time step size and the penalty value.

## 6 SUMMARY AND CONCLUSIONS

- The results of the validation study show that DDA solution of an idealized system for which an analytical solution exists, is accurate. The DDA intra-block contact algorithm is therefore a true replication of the analytical model for frictional sliding.
- The accuracy of DDA is governed by the conditioning of the stiffness matrix. DDA solution is accurate provided that the chosen time step is small enough to assure diagonal dominance of the global stiffness matrix.
- Numeric spring stiffness should be optimized in conjunction with the chosen time step size to assure accurate solution and to preclude ill conditioning of the global stiffness matrix.
- Comparison between a shaking table model and DDA calculation shows that the DDA solution is conservative. For accurate prediction of dynamic displacement of single block on an incline a reduction of the dynamic control parameter ( $kOI$ ) by 2% is recommended.

## 7 ACKNOWLEDGMENTS

This research is funded by the US – Israel Binational Science Foundation through grant 98-399. The authors wish to express their gratitude to Gen-hua Shi who kindly provided his new dynamic version of DDA. Shaking table data were provided by J. Wartman of Drexel University, R. Seed, and J. Bray of University of California, Berkeley, and their cooperation is greatly appreciated.

## REFERENCES

- Doolin, D & Sitar, N. 2001. Accuracy of the DDA method with respect to a single sliding block. In: *Rock Mechanics in the National Interest*, proceedings of the 38th U.S. Rock Mechanics Symposium, Washington D.C., July 5-7, 2001. Balkema, Rotterdam.



- Goodman, R. E. & Seed H. B. 1965. Earthquake induced displacements in sand embankments. *J. of Soil Mech. and Foundations Div. ASCE*. 92(SM2): 125– 146.
- Hatzor, Y. H. & Feintuch, A. 2001. The validity of dynamic block displacement prediction using DDA. *Int. J. of Rock Mech. and Min. Sci.* 38: 599 – 606.
- Kim, J., Bray, J. D., Reimer, M. F. & Seed. R. B. 1999. *Dynamic interface friction properties of geosynthetics*. Unpublished report, University of California at Berkeley, Department of Civil Engineering.
- MacLaughlin, M. 1997. *Discontinuous Deformation Analysis of the kinematics of rock slopes*. Ph.D. thesis, Department of Civil Engineering, University of California, Berkley.
- McBride, A., Scheele, F. 2001. Investigation of discontinuous deformation analysis using physical laboratory models. In: Bicanic, N. (ed.). *Proc. of the Fourth International Conference on Discontinuous Deformation Analysis*. 73-82. Glasgow, 6-8 June.
- Newmark, N. M. 1959. A method of computation for structural dynamics. *J. of the Eng. Mech. Div. ASCE* . 85(EM3)
- O’Sullivan, C. & Bray, J. D. 2001. A comparative evaluation of two approaches to discrete element modeling to particulate media. In: Bicanic, N. (ed.). *Proceedings of the Fourth International Conference on Discontinuous Deformation Analysis*. 97-110. Glasgow, 6-8 June.
- Shi, G-h. 1988. *Discontinuous Deformation Analysis – A new model for the statics and dynamics of block systems*. Ph.D. thesis, Department of Civil Engineering, University of California, Berkley.
- Shi, G-h. 1993. *Block system modeling by discontinuous deformation analysis*. In: Brebbia, C. A. & Connor, J. J. (eds). *Topics in Engineering*, Vol. 11. Computational Mechanics Publication.
- Shi, G-h. 1999. Applications of Discontinuous Deformation Analysis and Manifold method. In: Amadei, B (ed.). *Third International Conference on Analysis of Discontinuous Deformation*. 3-16. Vail, Colorado, 3 – 4 June.
- Wang, C-Y., Chuang C-C. & Sheng, J. 1996. Time integration theories for the DDA method with Finite Element meshes. In: Reza Salami, M. & Banks, M. (eds.). *Proceedings of the Firth International Forum on Discontinuous Deformation Analysis (DDA) and Simulation of Discontinuous Media*. 97-110. Berkeley, 12-14 June. TSI Press: Albuquerque.
- Wartman, J. 1999. *Physical model studies of seismically induced deformation in slopes*. Ph.D. thesis, Department of Civil Engineering, University of California, Berkley.
- Yeung, M. R. 1991. *Application of Shi’s DDA to the study of rock behavior*. Ph.D. thesis, Department of Civil Engineering, University of California, Berkley.